Chiroptical Absorption and Luminescence Spectra of a Dissymmetric Osmium(II)−Polypyridyl Complex Containing an Optically Active Bis(bipyridine)-Type Ligand of Well-Defined Structural Chirality

Kevin E. Gunde,[†] Alberto Credi,[†,‡] Erik Jandrasics,[§] Alex von Zelewsky,[§] and F. S. Richardson*,[†]

Department of Chemistry, University of Virginia, Charlottesville, Virginia 22901, and Institute of Inorganic Chemistry, University of Fribourg, Pérolles, CH-1700 Fribourg, Switzerland

Received July 26, 1996[⊗]

Chiroptical absorption and luminescence spectra are reported for a novel Os(II)−polypyridyl complex in which Os(II) is coordinated to one *achiral* bidentate ligand and a *chiral* quadridentate ligand. The achiral ligand is 4,4′-dimethyl-2,2′-bipyridine (DMbpy), and the chiral ligand is a bisbipyridine-type molecule formed by linking two optically active (−)-[4,5]-pineno-2,2′-bipyridine molecules together via a $(CH_2)_6$ chain bridge. This chiral ligand is one of a family of ligands often referred to as *chiragens*, and here it is denoted by CG[6], where [6] identifies the number of carbon atoms in the chain bridge. The coordination core of the complex has a three-bladed propeller-like structure formed by three Os(II)−bipyridyl chelate rings. This tris(bipyridyl)Os(II) core structure has approximate trigonal-dihedral (D_3) symmetry, and the propeller-like assembly of its three chelate rings has a right-handed screw sense (or helicity). The overall complex, denoted by Δ-[Os(CG[6])(DMbpy)]$^{2+}$, has C_2 point-group symmetry, with a 2-fold symmetry axis that bisects both the CG[6] and DMbpy ligands and coincides with one of the digonal (C_2) axes of the tris(bipyridyl)Os(II) core structure. The overall structural chirality of the complex is dictated by the inherent chirality of the CG[6] ligand, which in turn is dictated by the absolute configuration about each of the six stereogenic carbon atoms in the CG[6] ligand structure. The chiroptical absorption and luminescence measurements performed in this study were carried out on solution samples of Δ-[Os(CG[6])(DMbpy)]$(PF_6)_2$ dissolved in acetonitrile. These measurements yielded circular dichroism and absorption dissymmetry factor data over the 12 500−30 000 cm^{-1} spectral range, and circularly polarized luminescence and emission dissymmetry factor data over the 11 100−16 000 cm^{-1} spectral region. Comparisons between the absorption and emission dissymmetry factor data indicate chirality-related structural differences between the ground and emitting states of Δ-[Os(CG[6])(DMbpy)]$^{2+}$. Both the unpolarized and circularly polarized absorption spectra of Δ-[Os(CG[6])(DMbpy)]$^{2+}$ are *qualitatively* similar to the corresponding spectra reported for Δ-[Os(bpy)$_3$]$^{2+}$ (in acetonitrile) throughout the 12 500−30 300 cm^{-1} spectral region. However, there are significant *quantitative* differences between the spectra observed for these two complexes, and these differences are most apparent in the absorption dissymmetry factor data. This indicates that ligand structure outside the tris(bipyridyl)Os(II) coordination core of Δ-[Os(CG[6])(DMbpy)]$^{2+}$ exerts a significant influence on the chiroptical absorption properties of this complex over the 12 500−30 300 cm^{-1} spectral region, although all the optical absorption processes that occur within this spectral region may be assigned to one-electron d−π*-type metal-to-ligand charge-transfer (MLCT) transitions localized within the tris(bipyridyl)Os(II) chelate structure. It appears that the noncoordinated chiral moieties of the CG[6] ligand exert a direct perturbative influence on both the dipole strengths and rotatory strengths of the MLCT transitions in Δ-[Os(CG[6])(DMbpy)]$^{2+}$.

Introduction

Chiral transition-metal complexes have structural and reactivity properties that are of fundamental interest and practical importance in many areas of chemistry and biochemistry. Of special interest are those properties that exhibit a dependence on the degree and sense of structural chirality (or "handedness") in the complexes. These chirality-dependent properties are manifested in a wide variety of processes where the complexes are observed to exhibit chirality-related biases in their physical interactions and chemical reactions with other chiral (or prochiral) molecular species. They are also manifested in optical processes that involve the absorption or emission of circularly polarized light. Chiral metal complexes exhibit different absorption (and emission) probabilities for left- vs right-circularly polarized light, and these circular differential optical properties are a direct consequence of chirality in the electronic and stereochemical structures of the complexes.[1−5] The circular differential optical properties of a chiral system are often referred to as *chiroptical* properties, and measurements of these properties are used extensively in studies of molecular chirality and chirality-dependent molecular processes.[6−8]

[†] Department of Chemistry, University of Virginia.
[‡] Present address: Dipartimento di Chimica "G. Ciamician", Università di Bologna, via Selmi 2, 40126 Bologna, Italy.
[§] Institute of Inorganic Chemistry, University of Fribourg.
[⊗] Abstract published in *Advance ACS Abstracts,* January 1, 1997.

(1) Richardson, F. S. *Chem. Rev.* **1979**, *79*, 17−37.
(2) Saito, Y. *Inorganic Molecular Dissymmetry*; Springer-Verlag: Berlin, 1979.
(3) *Stereochemistry of Optically Active Transition Metal Compounds*; Douglas, B. E., Saito, Y., Eds.; ACS Symposium Series 119; American Chemical Society: Washington, DC, 1980.
(4) Jensen, H. P.; Woldbye, F. *Coord. Chem. Rev.* **1979**, *29*, 213−235.
(5) Radanovic, D. J. *Coord. Chem. Rev.* **1984**, *54*, 159−261.
(6) Barron, L. D. *Molecular Light Scattering and Optical Activity*; Cambridge University Press: Cambridge, UK, 1982.
(7) Mason, S. F. *Molecular Optical Activity and the Chiral Discriminations*; Cambridge University Press: Cambridge, UK, 1982.
(8) *Circular Dichroism. Principles and Applications*; Nakanishi, K., Berova, N., Woody, R. W., Eds.; VCH Publishers: New York, 1994.

S0020-1669(96)00901-9 CCC: $14.00

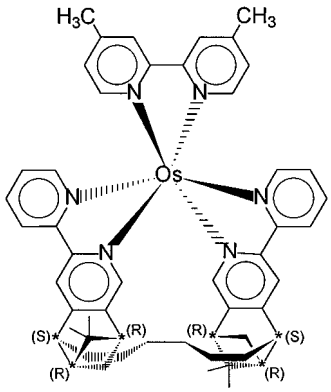

Figure 1. Schematic drawing of Δ-[Os((+)-chiragen[6])(4,4′-dimethyl-2,2′-bipyridine)]$^{2+}$, with the stereogenic carbon atoms identified by asterisks and their absolute configurations noted in parentheses.

In the present paper we report results obtained from chiroptical absorption and luminescence measurements performed on a novel Os(II)−polypyridyl complex that is dissymmetric (i.e., contains no improper rotation axes among its symmetry elements) and possesses several types of structural chirality. Using nomenclature and notation applied previously to the Ru(II) analogue of this complex,[9] we denote the complex as Δ-[Os((+)-chiragen[6])(4,4′-dimethyl-2,2′-bipyridine)]$^{2+}$, where (+)-chiragen[6] corresponds to a quadridentate ligand comprised of two (−)-[4,5]-pineno-2,2′-bipyridine molecules linked together via an aliphatic C_6-chain bridge. In this complex, Os(II) is coordinated to six nitrogen atoms: two from each of the bipyridyl moieties of the chiragen[6] ligand and two from the 4,4′-dimethyl-2,2′-bipyridine ligand. The complex has C_2 point-group symmetry, with a 2-fold symmetry axis that bisects the C_6-chain bridge of the chiragen[6] ligand and coincides with the 2-fold symmetry axis of the 4,4′-dimethyl-2,2′-bipyridine ligand. Structural representations of the complex are shown in Figures 1 and 2. These structural representations are based on structure data reported for Δ-[Ru((+)-chiragen[6])(4,4′-dimethyl-2,2′-bipyridine)]$(CF_3SO_3)_2$,[9] with adjustments made for Ru(II)-to-Os(II) substitution, using molecular mechanics calculations. Hereafter we will frequently use the more abbreviated notation Δ-[Os(CG[6])(DMbpy)]$^{2+}$ in referring to the Δ-[Os((+)-chiragen[6])(4,4′-dimethyl-2,2′-bipyridine)]$^{2+}$ complex examined in this study.

Each of the two pinene-substituted bipyridine subunits of the (+)-chiragen[6] ligand in Δ-[Os(CG[6])(DMbpy)]$^{2+}$ has three stereogenic carbon atoms, and the locations of these atoms are identified by asterisks in the structure shown in Figure 1. The absolute configuration at each of the two carbon atoms attached to the C_6-chain bridge between the [4,5]-pineno-2,2′-bipyridine subunits is *S*, and this *S*,*S* pair of stereogenic atomic centers in the (+)-chiragen[6] ligand dictates the configurational chirality of the chelate ring structure around the Os(II) metal center. The three Os(II)−bipyridyl chelate rings in this structure are arranged in the shape of a three-bladed propeller with a *right-handed* screw sense (or helicity) about its *pseudo*-C_3 symmetry axis. (Note that this propeller assembly does not have a *true* C_3 symmetry axis because its three blades are not fully equivalent.) The right-handed helicity of the tris(bipyridyl)Os(II) core structure in Δ-[Os(CG[6])(DMbpy)]$^{2+}$ is specified by the label Δ. This source of structural chirality in the complex is expected to play the dominant role in determining the chiroptical absorption and luminescence properties of the complex in the near-ultraviolet, visible, and near-infrared spectral regions.

(9) (a) Hayoz, P.; von Zelewsky, A.; Stoeckli-Evans, H. *J. Am. Chem. Soc.* **1993**, *115*, 5111−5114. (b) Jandrasics, E. Ph.D. Thesis 1085, University of Fribourg, Fribourg, Switzerland, 1995.

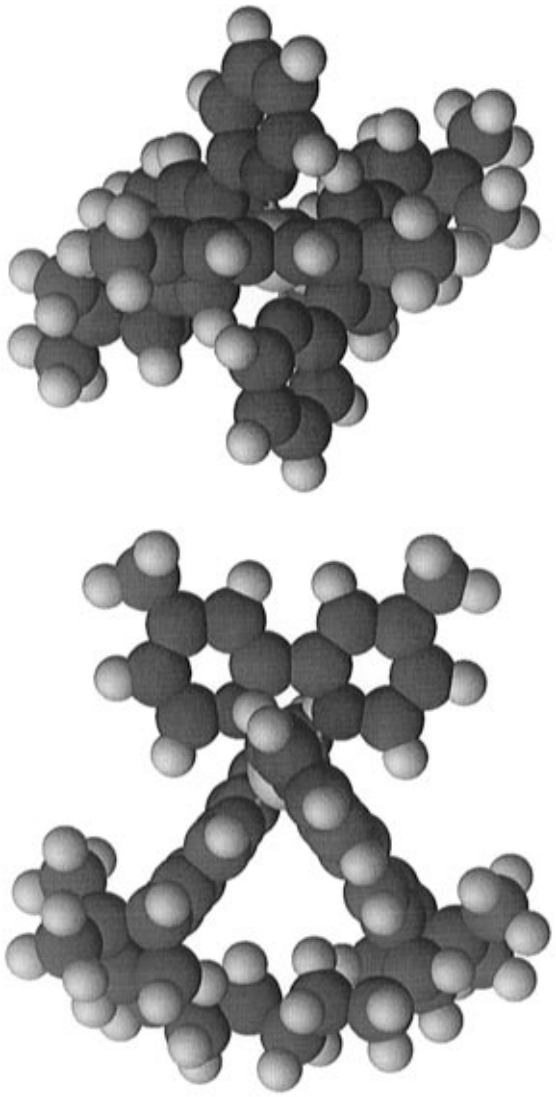

Figure 2. Structural representations of Δ-[Os((+)-chiragen[6])(4,4′-dimethyl-2,2′-bipyridine)]$^{2+}$. The upper view is along an axis which is *parallel* to the C_2 symmetry axis of the complex and the lower view is along an axis which is *perpendicular* to the C_2 symmetry axis of the complex.

All of the chiroptical absorption and luminescence measurements reported in this study were obtained on solution samples of Δ-[Os(CG[6])(DMbpy)]$(PF_6)_2$ dissolved in acetonitrile. The absorption measurements spanned the 330−800 nm wavelength region of the spectrum and were carried out under room-temperature conditions. The luminescence measurements spanned the 600−900 nm wavelength range and were carried out under conditions in which the sample temperature was maintained at 293 K and sample luminescence was excited by continuous-wave laser radiation at 488 nm.

Chiroptical absorption measurements have been used extensively in studies of chiral transition-metal complexes, but very few chiroptical luminescence measurements have been reported. The latter can be attributed in large part to the fact that not many transition-metal complexes exhibit a detectable luminescence in fluid solution media, but it is also due in part to a general unfamiliarity with chiroptical luminescence measurement techniques. In the following section we give brief descriptions of chiroptical absorption and luminescence measurement techniques and show how the observables in these two types of measurements are related to chirality-dependent molecular electronic and stereochemical properties.

Chiroptical Absorption and Luminescence Measurement Techniques

Chiroptical Absorption Spectra. In chiroptical absorption experiments, one measures sample absorptivities for left- and right-circularly polarized light to obtain the following quantities of special interest:

$$\epsilon(\bar{\nu}) = \frac{[\epsilon_L(\bar{\nu}) + \epsilon_R(\bar{\nu})]}{2} \quad \text{(mean absorptivity)} \tag{1}$$

$$\Delta\epsilon(\bar{\nu}) = \epsilon_L(\bar{\nu}) - \epsilon_R(\bar{\nu}) \quad \text{(circular dichroism)} \tag{2}$$

$$g_{ab}(\bar{\nu}) = \Delta\epsilon(\bar{\nu})/\epsilon(\bar{\nu}) \quad \text{(absorption dissymmetry factor)} \tag{3}$$

where $\epsilon_L(\bar{\nu})$ and $\epsilon_R(\bar{\nu})$ denote molar absorptivities for left (L)- and right (R)-circularly polarized light of wavenumber $\bar{\nu}$. These measurements are commonly referred to as circular dichroism (CD)/absorption measurements, and instrumentation for making these measurements over the near-infrared, visible, and near-to far-ultraviolet regions of the spectrum is commercially available. The results obtained from these measurements are typically displayed as ϵ vs $\bar{\nu}$ (*absorption*) and $\Delta\epsilon$ vs $\bar{\nu}$ (*CD*) spectra, which in the experiments of interest here show lines or bands associated with molecular electronic (and/or vibronic) transitions that originate from the equilibrium ground state of the molecular chromophores.

For samples in which the molecular chromophores are randomly oriented, the contributions of any given electronic transition (e.g., g $\rightarrow$ j) to the absorption (ϵ) and CD ($\Delta\epsilon$) spectra may, to a very good approximation, be expressed as

$$\epsilon(\bar{\nu}) = (KD_{gj}/d_g)[\bar{\nu}\chi(\bar{\nu})L^{\epsilon}_{gj}(\bar{\nu})] \tag{4}$$

$$\Delta\epsilon(\bar{\nu}) = (4KR_{gj}/d_g)[\bar{\nu}\bar{\chi}(\bar{\nu})L^{\Delta\epsilon}_{gj}(\bar{\nu})] \tag{5}$$

where K is a constant quantity defined by $8\pi^3N_A/3000hc \ln 10$ (which has a value of $\sim 1.089 \times 10^{38}$ in cgs units), d_g denotes the degeneracy of the ground electronic state (g), $\chi(\bar{\nu})$ and $\bar{\chi}(\bar{\nu})$ are factors dependent on the optical refractivity of the bulk sample medium, $L^{\epsilon}_{gj}(\bar{\nu})$ and $L^{\Delta\epsilon}_{gj}(\bar{\nu})$ are unit-normalized line shape functions centered within the spectral frequency distribution of the g $\rightarrow$ j transition, and D_{gj} and R_{gj} are transition line strength quantities defined by

$$D_{gj} = |\langle\psi_g|\boldsymbol{\mu}|\psi_j\rangle|^2 + |\langle\psi_j|\mathbf{m}|\psi_g\rangle|^2 \tag{6}$$

$$R_{gj} = \mathrm{Im}[\langle\psi_g|\boldsymbol{\mu}|\psi_j\rangle\cdot\langle\psi_j|\mathbf{m}|\psi_g\rangle] \tag{7}$$

where $\boldsymbol{\mu}$ and $\mathbf{m}$ denote, respectively, electric and magnetic dipole moment operators, ψ_g and ψ_j denote state vectors for the ground (g) and excited (j) electronic states in the g $\rightarrow$ j transition, and Im specifies the *imaginary* part of the quantity that follows. Hereafter, we shall refer to D_{gj} as a transition *dipole strength* and to R_{gj} as a transition *rotatory strength*. We note that for transitions that are fully resolved in the absorption and CD spectra, the D_{gj} and R_{gj} quantities may be determined from the experimental data by evaluating

$$D_{gj} = \frac{d_g}{K}\int_{g\rightarrow j}\frac{\epsilon(\bar{\nu})}{\chi(\bar{\nu})\bar{\nu}}\,d\bar{\nu} \quad \text{and} \quad R_{gj} = \frac{d_g}{4K}\int_{g\rightarrow j}\frac{\Delta\epsilon(\bar{\nu})}{\bar{\chi}(\bar{\nu})\bar{\nu}}\,d\bar{\nu} \tag{8}$$

where $\int_{g\rightarrow j}$ specifies integration over the spectral profile of the g $\rightarrow$ j transition.

The transition dipole strengths, defined according to eq 6, are scalar quantities with values that must be ≥ 0. On the other hand, the transition rotatory strengths, defined according to eq 7, are *pseudoscalar* quantities with values that may be 0, >0, or <0, depending on the relative orientations of the $\langle\psi_g|\boldsymbol{\mu}|\psi_j\rangle$ and $\langle\psi_j|\mathbf{m}|\psi_g\rangle$ transition vectors (or equivalently, the relative phases of the $\langle\psi_g|\boldsymbol{\mu}|\psi_j\rangle$ and $\langle\psi_j|\mathbf{m}|\psi_g\rangle$ transition amplitudes). If we denote the magnitudes of the $\langle\psi_g|\boldsymbol{\mu}|\psi_j\rangle$ and $\langle\psi_j|\mathbf{m}|\psi_g\rangle$ transition vectors as μ_{gj} and m_{jg}, respectively, and the angle between them as θ_{gj}, then eqs 6 and 7 may be rewritten as

$$D_{gj} = (\mu_{gj})^2 + (m_{jg})^2 \tag{9}$$

$$R_{gj} = \mu_{gj}m_{jg}\cos\theta_{gj} \tag{10}$$

and we note that the sign of R_{gj} is determined *entirely* by the value of θ_{gj}, and the magnitude of R_{gj} is also dependent on θ_{gj}. The magnitude and sign of the cos θ_{gj} function are determined by the degree and sense of helicity in the molecular force field that acts on the chromophoric electrons involved in the g $\rightarrow$ j transition, and the helicity of this force field is determined by the degree and sense of chirality in the ground-state stereochemical structure of the molecular chromphore. Opposite enantiomers of a chiral molecule show identical values of μ_{gj} and of m_{jg}, but they show θ_{gj} angles that differ by 180° and R_{gj} values that are equal in magnitude but opposite in sign.

Chiroptical Luminescence Spectra. There are many variations of chiroptical luminescence experiments, with the variations related mostly to different sample excitation techniques, luminophore orientational distribution properties, and excitation/emission detection geometries.[10−14] However, common to all the experiments are (1) collection of sample luminescence, (2) separation (or analysis) of the collected luminescence into circularly polarized components, and (3) measurements of the following quantities:

$$I(\bar{\nu}') = I_L(\bar{\nu}') + I_R(\bar{\nu}') \quad \text{(TL intensity)} \tag{11}$$

$$\Delta I(\bar{\nu}') = I_L(\bar{\nu}') - I_R(\bar{\nu}') \quad \text{(CPL intensity)} \tag{12}$$

$$g_{em}(\bar{\nu}') = \Delta I(\bar{\nu}')/I(\bar{\nu}')/2 \quad \text{(emission dissymmetry factor)} \tag{13}$$

where $I_L(\bar{\nu}')$ and $I_R(\bar{\nu}')$ denote intensities for the left (L)- and right (R)-circularly polarized components of the luminescence collected from the sample and measured at the emission wavenumber $\bar{\nu}'$. It has become standard practice to refer to $I(\bar{\nu}')$ as a total luminescence (TL) intensity and to $\Delta I(\bar{\nu}')$ as a circularly polarized luminescence (CPL) intensity, and we shall retain that practice here.

The chiroptical luminescence measurements performed in the present study were carried out under *steady-state* excitation/emission detection conditions, on solution samples in which the emitting-state population of molecules could be presumed to be rotationally relaxed and comprised of randomly oriented luminophores. Under these conditions, the contributions of any given electronic transition (e.g., g $\leftarrow$ i) to the TL (I) and CPL (ΔI) spectra may, to a very good approximation, be expressed as

(10) Richardson, F. S.; Riehl, J. P. *Chem. Rev.* **1977**, *77*, 773−794.
(11) Riehl, J. P.; Richardson, F. S. *Chem. Rev.* **1986**, *86*, 1−17.
(12) Dekkers, H. P. J. M. In *Circular Dichroism: Interpretation and Applications*; Nakanishi, K., Berova, N., Woody, R. W., Eds.; VCH Publishers: New York, 1994; Chapter 6, pp 121−152.
(13) Richardson, F. S.; Metcalf, D. H. In *Circular Dichroism: Interpretation and Applications*; Nakanishi, K., Berova, N., Woody, R. W., Eds.; VCH Publishers: New York, 1994; Chapter 7, pp 153−178.
(14) Riehl, J. P. In *Analytical Applications of Circular Dichroism*; Purdie, N., Brittain, H. G., Eds.; Elsevier: Amsterdam, 1994.

$$I(\bar{\nu}') = \frac{K'\bar{N}_i D'_{gi}}{d_i}[(\bar{\nu}')^4 \chi'(\bar{\nu}') L^{\ I}_{gi}(\bar{\nu}')] \tag{14}$$

$$\Delta I(\bar{\nu}') = \frac{2K'\bar{N}_i R'_{gi}}{d_i}[(\bar{\nu}')^4 \bar{\chi}'(\bar{\nu}') L^{\ \Delta I}_{gi}(\bar{\nu}')] \tag{15}$$

where $K' = 16\pi^3 c/3$ (if the intensity quantities are expressed in units of energy per second per unit solid angle), $\bar{N}_i$ is the concentration of molecules in the emitting state (i) under the steady-state excitation/emission conditions of the experiment, d_i denotes the degeneracy of the emitting state, $\chi'(\bar{\nu}')$ and $\bar{\chi}'(\bar{\nu}')$ are factors dependent on the optical refractivity of the bulk sample medium, and $L^{\ I}_{gi}(\bar{\nu}')$ and $L^{\ \Delta I}_{gi}(\bar{\nu}')$ are unit-normalized line shape functions centered within the spectral frequency distribution of the g ← i transition. The D'_{gi} and R'_{gi} quantities are defined by

$$\begin{aligned} D'_{gi} &= |\langle\psi'_g|\boldsymbol{\mu}|\psi'_i\rangle|^2 + |\langle\psi'_i|\mathbf{m}|\psi'_g\rangle|^2 \\ &= (\mu'_{gi})^2 + (m'_{ig})^2 \end{aligned} \tag{16}$$

$$\begin{aligned} R'_{gi} &= \mathrm{Im}[\langle\psi'_g|\boldsymbol{\mu}|\psi'_i\rangle\cdot\langle\psi'_i|\mathbf{m}|\psi'_g\rangle] \\ &= \mu'_{gi} m'_{ig} \cos\theta'_{gi} \end{aligned} \tag{17}$$

where except for the prime symbols, all the notation used in these equations corresponds (in meaning) to that used and defined earlier for eqs 6, 7, 9, and 10. The primes on the ψ'_g and ψ'_i wavefunctions indicate that these wave functions are eigenfunctions of a molecular Hamiltonian that reflects the geometry and stereochemical structure of the luminophores in their vibrationally relaxed emitting state (i). In contrast, the ψ_g and ψ_j wave functions specified in eqs 6 and 7, which pertain to absorption processes, are defined to be eigenfunctions of a molecular Hamiltonian that reflects the geometry and stereochemical structure of the chromophores in their equilibrium ground state. The use of prime labels on the μ'_{gi}, m'_{jg}, θ'_{gi}, D'_{gi}, and R'_{gi} quantities in eqs 16 and 17 follows from the dependence of these quantities on ψ'_g and ψ'_i.

Absorption and Emission Dissymmetry Factors. Insertion of eqs 4 and 5 into eq 3 yields the following expression for the absorption dissymmetry factor measured within the g → j electronic transition region:

$$g_{ab}(\bar{\nu}) = \frac{4R_{gj}}{D_{gj}}\left[\frac{\bar{\chi}(\bar{\nu}) L^{\ \Delta\epsilon}_{gj}(\bar{\nu})}{\chi(\bar{\nu}) L^{\ \epsilon}_{gj}(\bar{\nu})}\right] = \frac{4R_{gj}}{D_{gj}} G_{gj}(\bar{\nu}) \tag{18}$$

For fully resolved transitions, it is generally observed that the CD ($\Delta\epsilon$) and absorption (ϵ) bands that contribute to $g_{ab}(\bar{\nu})$ have very similar shapes and baricenter locations, and g_{ab} is essentially constant over the spectral profile of any given transition. This suggests that the $G_{gj}(\bar{\nu})$ function in eq 18 may be replaced with a constant factor which, to a reasonably good approximation, can be assumed to represent the ratio of $\bar{\chi}(\bar{\nu})$ to $\chi(\bar{\nu})$, evaluated at the baricenter frequency of the g → j absorption band. If it is further assumed that $\bar{\chi}(\bar{\nu})$ and $\chi(\bar{\nu})$ derive from Lorentz-type local field corrections, then eq 18 may be rewritten as

$$g_{ab}(\mathrm{g}\rightarrow\mathrm{j}) \cong \frac{4R_{gj}\bar{\chi}}{D_{gj}\chi} \tag{19a}$$

$$\cong \frac{4[(n^2+2)/3]\mu_{gj} m_{jg} \cos\theta_{gj}}{[(n^2+2)^2/9n](\mu_{gj})^2 + n(m_{jg})^2} \tag{19b}$$

where n denotes the refractive index of the bulk sample medium at the optical frequency of interest. For the great majority of electronic transitions observed in noncentrosymmetric molecular systems, one may assume that $\mu_{gj} \gg m_{jg}$, in which case eq 19b reduces to

$$g_{ab}(\mathrm{g}\rightarrow\mathrm{j}) \cong 4\left[\frac{3n}{n^2+2}\right]\frac{m_{jg}\cos\theta_{gj}}{\mu_{gj}} \tag{20}$$

Insertion of eqs 14 and 15 into eq 13 yields the following expression for the emission dissymmetry factor measured within the g ← i transition region:

$$g_{em}(\bar{\nu}') = \frac{4R'_{gi}}{D'_{gi}}\left[\frac{\bar{\chi}'(\bar{\nu}') L^{\ \Delta I}_{gi}(\bar{\nu}')}{\chi'(\bar{\nu}') L^{\ I}_{gi}(\bar{\nu}')}\right] = \frac{4R'_{gi}}{D'_{gi}} G'_{gi}(\bar{\nu}') \tag{21}$$

Similar to the behavior noted above for absorption dissymmetry factors, the g_{em} factors determined from CPL (ΔI) and TL (I) measurements generally show very little variation with frequency within any given transition region. If we apply the same conditions and approximations to eq 21 that we applied above to eq 18, we obtain

$$g_{em}(\mathrm{g}\leftarrow\mathrm{i}) \cong 4R'_{gi}\bar{\chi}'/D'_{gi}\chi' \tag{22a}$$

$$\cong \frac{4[n^2(n^2+2)/3]\mu'_{gi} m'_{ig} \cos\theta'_{gi}}{[n(n^2+2)^2/9](\mu'_{gi})^2 + n^3(m'_{ig})^2} \tag{22b}$$

where n denotes the refractive index of the bulk sample medium at the optical emission frequency of the g ← i transition. In cases where it may be assumed that $\mu'_{gi} \gg m'_{ig}$, expression 22b reduces to

$$g_{em}(\mathrm{g}\leftarrow\mathrm{i}) \cong 4\left[\frac{3n}{n^2+2}\right]\frac{m'_{ig}\cos\theta'_{gi}}{\mu'_{gi}} \tag{23}$$

In the special case where CD/absorption measurements are performed throughout a transition region that corresponds to *direct* excitation of the luminescent electronic state (i), we may write

$$\frac{g_{em}(\mathrm{g}\leftarrow\mathrm{i})}{g_{ab}(\mathrm{g}\rightarrow\mathrm{i})} \cong \frac{R'_{gi}D_{gi}}{R_{gi}D'_{gi}}\left[\frac{\bar{\chi}'\chi}{\bar{\chi}\chi'}\right] \tag{24}$$

If we assume $\mu_{gj} \gg m_{jg}$ and $\mu'_{gi} \gg m'_{ig}$, this ratio may be re-expressed as

$$\frac{g_{em}(\mathrm{g}\leftarrow\mathrm{i})}{g_{ab}(\mathrm{g}\rightarrow\mathrm{i})} \cong \frac{|\langle\psi_g|\boldsymbol{\mu}|\psi_i\rangle||\langle\psi'_i|\mathbf{m}|\psi'_g\rangle|\cos\theta'_{gi}}{|\langle\psi'_g|\boldsymbol{\mu}|\psi'_i\rangle||\langle\psi_i|\mathbf{m}|\psi_g\rangle|\cos\theta_{gi}} \tag{25a}$$

$$\cong \frac{\mu_{gi} m'_{ig}\cos\theta'_{gi}}{\mu'_{gi} m_{ig}\cos\theta_{gi}} \tag{25b}$$

Any deviations of this ratio from a value of 1 (unity) are diagnostic of chirality-related differences between the stereochemical structures of a molecule in its emitting state and equilibrium ground state.

In CD/absorption experiments, one can generally measure the absolute values of $\epsilon_L(\bar{\nu})$ and $\epsilon_R(\bar{\nu})$ with reasonably good accuracy and then determine the absolute values of $\epsilon(\bar{\nu})$, $\Delta\epsilon(\bar{\nu})$, and $g_{ab}(\bar{\nu})$. The latter may then be used to determine the values of D_{gj}, R_{gj}, and $g_{ab}(\mathrm{g}\rightarrow\mathrm{j})$ from the relationships shown above in eqs 8 and 18. In chiroptical luminescence experiments, one generally measures only the relative values of $I_L(\bar{\nu}')$ and $I_R(\bar{\nu}')$, and then reports $I(\bar{\nu}')$ and $\Delta I(\bar{\nu}')$ in some arbitrarily chosen set of intensity units. This precludes the quantitative evaluation of D'_{gi} and R'_{gi} from the luminescence intensity data, but it permits the direct determination of $g_{em}(\bar{\nu}')$ values and, therefore, $g_{em}(\mathrm{g}\leftarrow\mathrm{i})$.

Chiroptical Spectra of Overlapping Electronic Transition Manifolds. In the preceding sections we focused primarily on the chiroptical properties of individual electronic transitions and showed how these properties can be evaluated from CD/absorption and CPL/emission data when the transitions appear as well-resolved (or resolvable) lines or bands in the optical absorption and emission spectra. However, in many cases the latter conditions are not met and the features observed in the relevant spectra represent convolutions of contributions from multiple transitions. This situation is encounterd in the CD/absorption spectra observed for Δ-[Os(CG[6])(DMbpy)]$^{2+}$ throughout the 12 500−30 000 cm^{-1} wavenumber region, and it is also relevant to the CPL/emission spectra observed for this complex.

If we consider the absorption (ϵ) and CD ($\Delta\epsilon$) spectra generated by a set of transitions g → {j}, all of which originate from the same ground state (g), we may write, by extensions of eqs 4 and 5,

$$\epsilon(\bar{\nu}') = \frac{K\bar{\nu}\chi(\bar{\nu})}{d_g}\sum_j D_{gj} L^{\epsilon}_{gj}(\bar{\nu}') \tag{26}$$

$$\Delta\epsilon(\bar{\nu}) = \frac{4K\bar{\nu}\bar{\chi}(\bar{\nu})}{d_g}\sum_j R_{gj} L^{\Delta\epsilon}_{gj}(\bar{\nu}) \tag{27}$$

$$g_{ab}(\bar{\nu}) = \frac{\Delta\epsilon(\bar{\nu})}{\epsilon(\bar{\nu})} = \frac{4\bar{\chi}(\bar{\nu})\sum_j R_{gj} L^{\Delta\epsilon}_{gj}(\bar{\nu})}{\bar{\chi}(\bar{\nu})\sum_j D_{gj} L^{\epsilon}_{gj}(\bar{\nu})} \tag{28}$$

If we assume that $L^{\Delta\epsilon}_{gj}(\bar{\nu})$ is essentially identical to $L^{\epsilon}_{gj}(\bar{\nu})$ for each of the transitions, then eqs 26−28 may be re-expressed as

$$\epsilon(\bar{\nu}) = (K/d_g)\sum_j D_{gj} F_{gj}(\bar{\nu}) \tag{29}$$

$$\Delta\epsilon(\bar{\nu}) = (K/d_g)\sum_j g_{ab}(g{\rightarrow}j) D_{gj} F_{gj}(\bar{\nu}) \tag{30}$$

$$g_{ab}(\bar{\nu}) = \sum_j g_{ab}(g{\rightarrow}j) D_{gj} L^{\epsilon}_{gj}(\bar{\nu}) \Big/ \sum_j D_{gj} L^{\epsilon}_{gj}(\bar{\nu}) \tag{31}$$

where $F_{gj}(\bar{\nu}) = \bar{\nu}\chi(\bar{\nu}) L^{\epsilon}_{gj}(\bar{\nu})$, and $g_{ab}(g \rightarrow j)$ is defined by eq 19. It is readily apparent from these expressions that the spectral profiles of $\epsilon(\bar{\nu})$, $|\Delta\epsilon(\bar{\nu})|$, and $|g_{ab}(\bar{\nu})|$ can be quite different over frequency regions that encompass multiple, overlapping transitions with different dissymmetry factors.

Electronic-State Structure of [Os(CG[6])(DMbpy)]$^{2+}$. The electronic states of direct relevance to the spectroscopic measurements performed in this study include the ground state and all excited states that are located between 12 500 and 30 000 cm^{-1} above ground. The electronic state structure of [Os(CG-[6])(DMbpy)]$^{2+}$ between 0 and 30 000 cm^{-1} is expected to be qualitatively similar to that of the well-studied [Os(bpy)$_3$]$^{2+}$ complex, in which case most (if not all) of the excited states located below 30 000 cm^{-1} may be assigned as one-electron d−π* type metal-to-ligand charge-transfer (MLCT) states.[15−20] In the ground state, three of the five 5d orbitals of Os(II) are doubly occupied, forming a 5d^6 singlet configuration, and the excited states of interest here are those formed by transferring an electron from any one of these occupied 5d orbitals to an empty π* orbital of the coordinated bpy moieties. If we restrict our attention only to those states formed by electron transfer into the *lowest energy* π* orbitals of the three coordinated bpy moieties, then the total number of MLCT states that may be formed is 36, 9 of which have principally *spin−singlet* parentage and 27 of which have principally *spin−triplet* parentage. Ferguson and Herren[16] discussed the energies and spin−orbital compositions of these states for [Os(bpy)$_3$]$^{2+}$, and they also discussed the likely contributions of these states to the optical absorption, CD, and luminescence spectra observed for [Os-(bpy)$_3$]$^{2+}$ at energies between 24 000 and 12 000 cm^{-1}. The energy-level structure associated with these states is too complex to permit definitive determinations of the locations and assignments of individual levels (from the observed spectra), but Ferguson and Herren did succeed in rationalizing many aspects of the observed spectra. Other workers have also examined the d−π* MLCT spectra of [Os(bpy)$_3$]$^{2+}$ in some detail,[15,17−23] and there is general agreement that all transitions that contribute to the optical absorption and luminescence spectra at energies of <18 000 cm^{-1} involve MLCT states of predominantly spin−triplet parentage and that the major contributions to the optical absorption spectrum between 18 000 and 24 000 cm^{-1} are from transitions that involve MLCT states of predominantly spin−singlet parentage. Moreover, it is generally agreed that the room-temperature luminescence spectrum of [Os(bpy)$_3$]$^{2+}$ includes contributions from at least three closely spaced emitting levels.

The d−π* MLCT state structure of [Os(CG[6])(DMbpy)]$^{2+}$ is expected to be very similar to that of [Os(bpy)$_3$]$^{2+}$, although there will be differences due to the lower symmetry of [Os-(CG[6])(DMbpy)]$^{2+}$ vs [Os(bpy)$_3$]$^{2+}$ (C_2 vs D_3 point-group symmetry) and small differences between the ligand π* acceptor orbitals in the two complexes. The lower symmetry of [Os-(CG[6])(DMbpy)]$^{2+}$ will remove many of the degeneracies predicted among the d−π* MLCT states of [Os(bpy)$_3$]$^{2+}$, and it is also likely to lead to either enhancements or redistributions of transition intensities in the d−π* MLCT absorption spectra. Ferguson and Herren[16] considered the effects of C_2 perturbations on the spectra of [Os(bpy)$_3$]$^{2+}$ contained in a [Zn(bpy)$_3$](PF$_6$)$_2$ host crystal, and they found clear evidence that these effects are manifested in the polarized intensity data of the system.

Results and Discussion

Absorption and Circular Dichroism Spectra. Absorption (ϵ) and CD ($\Delta\epsilon$) spectra measured over the 12 500−30 300 cm^{-1} spectral range are shown in Figure 3. These spectra were obtained at room temperature (∼293 K) on a 0.528 mM solution sample of Δ-[Os(CG[6])(DMbpy)](PF$_6$)$_2$ dissolved in acetonitrile. Also shown in Figure 3 is a line spectrum of g_{ab} values measured at the locations of maxima, minima, and shoulder features observed in the CD spectrum. The locations and properties of the eight features labeled as **1**−**8** are listed in Table 1.

The absorption and CD spectra shown in Figure 3 are qualitatively very similar to those reported recently for Δ-[Os-

(15) Pankuch, B. J.; Lacky, D. E.; Crosby, G. A. *J. Phys. Chem.* **1980**, *84*, 2061−2067.
(16) Ferguson, J.; Herren, F. *Chem. Phys.* **1983**, *76*, 45−59.
(17) Kober, E. M.; Meyer, T. J. *Inorg. Chem.* **1984**, *23*, 3877−3886.
(18) Caspar, J. V.; Westmoreland, T. D.; Allen, G. H.; Bradley, P. G.; Meyer, T. J.; Woodruff, W. H. *J. Am. Chem. Soc.* **1984**, *106*, 3492−3500.
(19) Ferguson, J.; Herren, G.; Krausz, E. R.; Maeder, M.; Vrbancich, J. *Coord. Chem. Rev.* **1985**, *64*, 21−39.
(20) Meyer, T. J. *Pure Appl. Chem.* **1986**, *58*, 1193−1206.
(21) Ferguson, J.; Herren, F.; McLaughlin, G. M. *Chem. Phys. Lett.* **1982**, *89*, 376−380.
(22) Giuffrida, G.; Calogero, G.; Guglielmo, G.; Ricevuto, V.; Ciano, M.; Campagna, S. *Inorg. Chem.* **1993**, *32*, 1179−1183.
(23) Riesen, H.; Wallace, L.; Krausz, E. *J. Chem. Phys.* **1995**, *102*, 4823−4831.

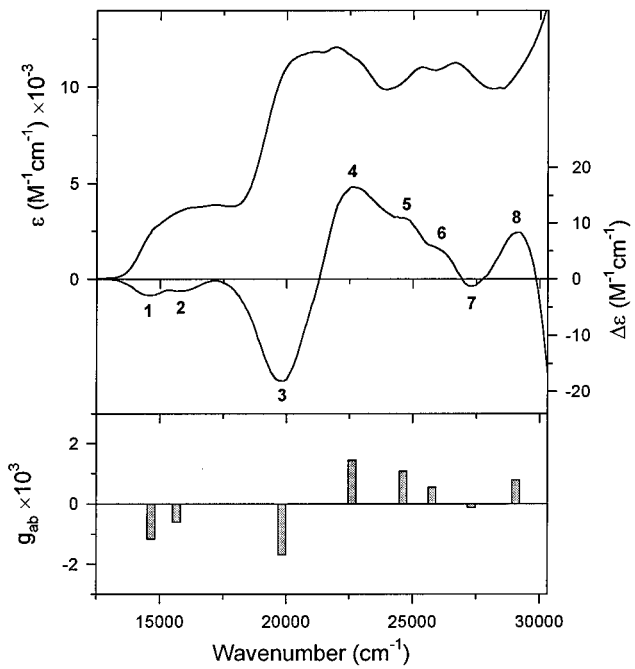

Figure 3. Absorption (ϵ) and CD ($\Delta\epsilon$) spectra obtained from measurements on a 0.528 mM solution sample of Δ-[Os(CG[6])-(DMbpy)](PF$_6$)$_2$ in acetonitrile. The bottom panel shows absorption dissymmetry factors ($g_{ab} = \Delta\epsilon/\epsilon$) measured at the locations of maxima, minima, and shoulder features (labeled as **1**−**8**) in the CD spectrum. All measurements were performed at a sample termperature of ∼293 K (room temperature).

Table 1. Locations and Properties of the Maxima, Minima, and Shoulder Features Observed in the CD Spectrum of Δ-[Os(CG[6])(DMbpy)]$^{2+}$ over the 12 500−30 300 cm^{-1} Spectral Range[a]

CD spectra features			$\Delta\epsilon$	ϵ	
label[b]	type[c]	location (cm^{-1})	(M^{-1} cm^{-1})	(M^{-1} cm^{-1})	$g_{ab} \times 10^3$
1	min	14 659	−2.87	2 488	−1.16
2	min	15 868	−2.09	3 599	−0.58
3	min	19 836	−18.08	10 676	−1.69
4	max	22 618	16.58	11 562	1.43
5	sh	24 624	10.99	10 278	1.07
6	sh	25 766	5.95	10 890	0.55
7	min	27 315	−1.27	10 601	−0.12
8	max	29 061	8.32	10 671	0.78

[a] All data are from CD/absorption measurements performed on a 0.528 mM solution sample of Δ-[Os(CG[6])(DMbpy)]$^{2+}$ in acetonitrile, at room temperature (∼293 K). See spectra shown in Figure 3. [b] Labels assigned according to Figure 3. [c] Features identified as minima (min), maxima (max), or shoulders (sh).

(bpy)$_3$]$^{2+}$ in acetonitrile solution.[24] The spectral features observed in the absorption and CD spectra of Δ-[Os(CG[6])-(DMbpy)]$^{2+}$ are red-shifted by ∼400 cm^{-1} from the corresponding features in the Δ-[Os(bpy)$_3$]$^{2+}$ spectra, but the shapes, relative intensities, spacings, and sign patterns of these features are very similar in the spectra of the two systems. However, significant differences are observed in the *absolute* values of ϵ, $\Delta\epsilon$, and g_{ab} measured for the two systems. Over the 14 000−18 000 cm^{-1} spectral region, the absorption spectrum of Δ-[Os-(CG[6])(DMbpy)]$^{2+}$ shows ϵ values that are ∼40% larger than those observed for Δ-[Os(bpy)$_3$]$^{2+}$, but the CD bands observed for Δ-[Os(CG[6])(DMbpy)]$^{2+}$ are only ∼40% as intense as those observed for Δ-[Os(bpy)$_3$]$^{2+}$. These results yield $|g_{ab}|$ values for Δ-[Os(CG[6])(DMbpy)]$^{2+}$ that, on average, are less than 30% as large as those for Δ-[Os(bpy)$_3$]$^{2+}$ over the 14 000−18 000 cm^{-1} spectral region. Similar differences between Δ-[Os(CG[6])(DMbpy)]$^{2+}$ and Δ-[Os(bpy)$_3$]$^{2+}$ are also observed in the absorption and CD intensity data acquired over the 19 000−30 000 cm^{-1} spectral region. Overall, the total oscillator strength of the d−π* MLCT transitions in Δ-[Os(CG[6])-(DMbpy)]$^{2+}$ is ∼40% larger than that observed for the same set of transitions in Δ-[Os(bpy)$_3$]$^{2+}$, but Δ-[Os(bpy)$_3$]$^{2+}$ exhibits stronger circular dichroism and absorption dissymmetry throughout the d−π* MLCT transition regions. We note, however, that the *net* (algebraically summed) CD intensity measured over the 12 500−30 000 cm^{-1} spectral region is very nearly zero for both Δ-[Os(CG[6])(DMbpy)]$^{2+}$ and Δ-[Os(bpy)$_3$]$^{2+}$. This implies that the total (*net*) rotatory strength associated with the d−π* MLCT transition manifold in each complex has a value close to zero.

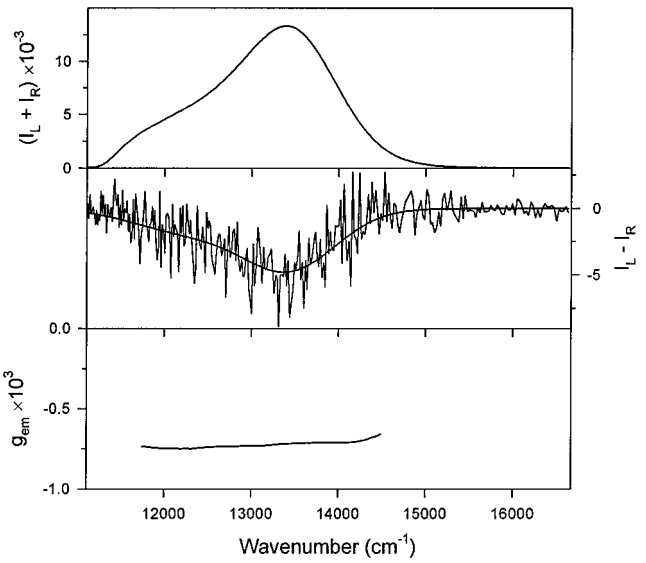

Figure 4. TL ($I = I_L + I_R$) and CPL ($\Delta I = I_L - I_R$) spectra obtained for Δ-[Os(CG[6])(DMbpy)]$^{2+}$ in acetonitrile solution (at 293 K). The noisy CPL trace represents the raw data obtained from the CPL measurements, and the smooth solid line CPL trace represents a fit of the raw data to the intensity distribution function defined by eq 33 in the text. The bottom panel shows a plot of emission dissymmetry factors ($g_{em} = 2\Delta I/I$) determined over the 11 750−14 500 cm^{-1} spectral region.

Luminescence Spectra. The TL ($I = I_L + I_R$) and CPL ($\Delta I = I_L - I_R$) spectra measured for Δ-[Os(CG[6])(DMbpy)]$^{2+}$ in acetonitrile solution (at 293 K) are shown in Figure 4 along with a plot of the corresponding emission dissymmetry factors (g_{em}). These spectra are not corrected to reflect the frequency-dependent emission-detection response of our instrumentation, which falls off rapidly on the far-red side of the emission spectrum (past 12 000 cm^{-1}). This, of course, does not affect the emission dissymmetry factor data, which correspond to ratios of ΔI to $I/2$ measured across the spectrum. Both "raw" and "smoothed" CPL spectra are shown in Figure 4, and all the ΔI data used in generating the $g_{em}(\bar{\nu}')$ plot were taken from the "smoothed" CPL spectrum.

The TL spectrum shown in Figure 4 is red-shifted by ∼400 cm^{-1} from the corresponding unpolarized luminescence spectrum reported for Δ-[Os(bpy)$_3$]$^{2+}$ in acetonitrile solution,[24] but otherwise these two spectra have very similar appearances. So far as we are aware, no CPL spectrum of Δ-[Os(bpy)$_3$]$^{2+}$ has yet been reported in the literature.

Both the TL and CPL spectra shown in Figure 4 are well represented by linear combinations of two Gaussian band shape functions: one (f_1) centered at 13 425 cm^{-1} with a half-width of 648 cm^{-1}, and the other (f_2) centered at 12 203 cm^{-1} with a half-width of 690 cm^{-1}. Expressed in terms of these functions,

(24) Noble, B.; Peacock, R. D. *Inorg. Chem.* **1996**, *35*, 1616−1620.

the observed TL and CPL spectra are given, to a very good approximation, by

$$I(\bar{\nu}') = N^{TL}[f_1(\bar{\nu}') + 0.345f_2(\bar{\nu}')] \quad (32)$$

$$\Delta I(\bar{\nu}') = -N^{CPL}[f_1(\bar{\nu}') + 0.348f_2(\bar{\nu}')] \quad (33)$$

where N^{TL} and N^{CPL} are intensity normalization factors which, for the spectra shown in Figure 4, are given by $N^{TL} = 2.77 \times 10^3$ $N^{CPL} = 1.274 \times 10^4$. A plot of eq 33, with N^{CPL} set equal to 4.60, yields the "smoothed" CPL spectrum shown in Figure 4.

It is reasonable to assume that the luminescence of [Os(CG-[6])(DMbpy)]$^{2+}$ originates from electronic and vibronic states that are very similar to those that contribute to the luminescence of [Os(bpy)$_3$]$^{2+}$. Analyses of [Os(bpy)$_3$]$^{2+}$ luminescence spectra indicate that, at room temperature, the observed emission occurs from a thermally equilibrated excited-state manifold comprised of at least three closely spaced ^{3}MLCT electronic states and their thermally accessible vibrational levels.[16,17] (Note that here we use the notation ^{3}MLCT to indicate a metal-to-ligand charge-transfer state with predominantly *spin−triplet* character.) Similar to the TL spectrum observed for [Os(CG[6])(DMbpy)]$^{2+}$(see Figure 4 and eq 32), the room-temperature luminescence spectrum of [Os(bpy)$_3$]$^{2+}$ in solution shows just two discernible features[24] that together may be represented by an intensity distribution function similar in form to that defined by our eq 32. It is generally assumed that the higher energy (and more intense) feature in this spectrum encompasses all of the "true" and "false" origin lines associated with transitions out of the emitting-state manifold and that the lower energy (and less intense) feature in the spectrum is comprised entirely of vibronic lines with origins located within the spectral band envelope of the higher energy feature. The luminescence spectrum of [Os-(CG[6])(DMbpy)]$^{2+}$ may be similarly interpreted, although the energy-level structure within the emitting-state manifold of this complex is likely to be more complicated than that of [Os-(bpy)$_3$]$^{2+}$.

We note from Figure 4 that emission dissymmetry, defined as $g_{em} = 2(I_L - I_R)/(I_L + I_R)$, is essentially constant across the luminescence spectrum of Δ-[Os(CG[6])(DMbpy)]$^{2+}$. This indicates that the rotatory strength-to-dipole strength ratios in the origin transitions are replicated in the vibronic transition manifolds, which further implies that the relevant electronic rotatory strength and dipole strength quantities have an essentially identical dependence on nuclear vibrational motions.

Comparisons between Chiroptical Absorption and Luminescence Spectra in the Overlapping Transition Regions. In Figure 5 we show the TL and CPL spectra of Δ-[Os(CG-[6])(DMbpy)]$^{2+}$ alongside the absorption and CD spectra measured over the ^{3}MLCT transition region. Also shown are the absorption dissymmetry factors (g_{ab}) measured at the locations of features **1** and **2** in the CD spectrum (see Figure 3 and Table 1) and the emission dissymmetry factors (g_{em}) measured at 13 425 (**1′**) and 12 203 cm^{-1} (**2′**), which correspond respectively to the centroids of the $f_1(\bar{\nu}')$ and $f_2(\bar{\nu}')$ functions in eqs 32 and 33. The values of these dissymmetry factors, as well as those measured at the midpoint between **1** and **1′**, are summarized in Table 2.

As was noted earlier, the absorption and CD spectra observed for Δ-[Os(bpy)$_3$]$^{2+}$ over the ^{3}MLCT transition region are qualitatively very similar to those observed for Δ-[Os(CG[6])-(DMbpy)]$^{2+}$ (and shown in Figure 5). In their interpretation of the Δ-[Os(bpy)$_3$]$^{2+}$ spectra, Ferguson and Herren[16] proposed that only one of the several (or many) ^{3}MLCT states that

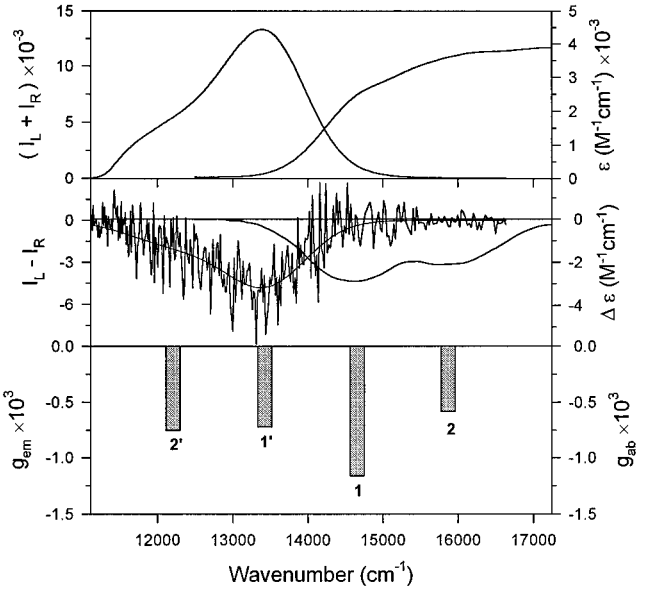

Figure 5. TL ($I = I_L + I_R$) and CPL ($\Delta I = I_L - I_R$) spectra and absorption (ϵ) and CD ($\Delta\epsilon$) spectra measured over the 11 100−17 200 cm^{-1} spectral region. The bottom panel shows emission dissymmetry factors measured at 12 203 cm^{-1} (**2′**) and 13 425 cm^{-1} (**1′**) and absorption dissymmetry factors measured at 14 659 (**1**) and 15 868 cm^{-1} (**2**).

Table 2. Absorption and Emission Dissymmetry Factors Measured at Special Points within the 12 000−17 000 cm^{-1} Spectral Region[a]

	wavenumber (cm^{-1})				
	12 203	13 425	14 042	14 659	15 868
$g_{em} \times 10^3$	−0.75	−0.72	−0.71		
$g_{ab} \times 10^3$			−1.85	−1.16	−0.58

[a] See relevant CD/absorption and CPL/emission spectra shown in Figures 3−5.

contribute to the absorption spectrum makes a detectable contribution to the CD spectrum. This would explain the distinctly different intensity profiles observed in the absorption vs CD spectra over the ^{3}MLCT transiton region. It would also require that the CD band we label as **2** in Figure 3 be assigned as the first member of a vibrational progression based on origin lines located within the CD band labeled as **1**. The separation between these bands (**1** and **2**) in the CD spectrum of Δ-[Os-(CG[6])(DMbpy)]$^{2+}$ is ∼1210 cm^{-1}, which may be compared to a separation of ∼1300 cm^{-1} between the corresponding bands in the CD spectrum of Δ-[Os(bpy)$_3$]$^{2+}$ (in solution).[24]

The two components of the "fitted" CPL spectrum, represented by eq 33, show a separation of 1222 cm^{-1}, and as was noted earlier the lower energy component (labeled here as **2′**) may be assigned as the first member of a vibrational progression based on origin lines located within the higher energy component (labeled here as **1′**). We further note from Figure 5 that the higher energy component (**1′**) of the CPL spectrum exhibits significant overlap with the lower energy component (**1**) of the CD spectrum, which suggests that the origin lines in the CPL and CD spectra may derive from identical electronic states. However, the differences between the g_{em} and g_{ab} values observed across the CPL and CD spectra (see values listed in Table 2) confound this picture.

The absorption and emission dissymmetry factors have identical signs throughout the CD−CPL spectral overlap region (15 000−13 000 cm^{-1}), but the values of g_{ab} are on average ∼2.5 times larger in magnitude than the values of g_{em}. This implies that the *degree* of structural chirality (or helicity) in the equilibrium ground state of Δ-[Os(CG[6])(DMbpy)]$^{2+}$

differs significantly from that in the emitting states. It is likely that this chirality-related difference between the ground- and emitting-state structures of Δ-[Os(CG[6])(DMbpy)]$^{2+}$ involves nuclear displacements that are distinct from those responsible for the Stokes shift observed in the luminescence/absorption spectra shown in Figure 5. The Stokes shift most likely reflects an isotropic radial expansion of the complex in its excited (emitting) states, whereas the differences between g_{em} and g_{ab} most likely reflect "twist-type" distortions between the ground- and excited-state structures of the complex.

For all the optical transitions of interest in this study, the relevant chromophoric unit of Δ-[Os(CG[6])(DMbpy)]$^{2+}$ is the trisbidentate chelate structure formed by the coordination of Os(II) to three bipyridyl ligand moieties. The three chelate rings in this structure are arranged in the shape of a three-bladed propeller with a right-handed screw sense (or helicity). The *degree* of helicity in this structure is defined by the *pitch* of the helix formed by the three chelate rings. A change in the screw sense of this helix (from right-handed to left-handed) is forbidden by structural constraints imposed by the extrachromophoric parts of the CG[6] ligand in [Os(CG[6])(DMbpy)]$^{2+}$.[9] However, changes in the pitch of the helix are expected to accompany any excitation or relaxation processes that alter the sizes of the chelate rings and/or the interactions between the chelate rings. Given the large redistribution of charge that occurs in a MLCT transition, it is reasonable to expect that the degree of helicity in the ^{3}MLCT emitting-state structure of Δ-[Os(CG[6])(DMbpy)]$^{2+}$ will differ from that in the equilibrium ground-state structure. This "twist-type" distortion between the ground- and emitting-state structures would lead to differences between the *magnitudes* of the g_{ab} and g_{em} values measured throughout the CD-CPL spectral overlap region.

The above discussion provides only a *qualitative* rationale for the spectra shown in Figure 5. A more detailed interpretation of the spectra would require considerably more information about the ^{3}MLCT energy-level structure in Δ-[Os(CG[6])(DMbpy)]$^{2+}$. Previous work on [Os(bpy)$_3$]$^{2+}$ provides useful clues about this energy-level structure, but many of the important details remain obscure. Differences between ground- and emitting-state chiroptical properties have been observed previously in several classes of optically active organic compounds[12] *and* in crystals of sodium uranyl acetate, Na[UO$_2$(CH$_3$COO)$_3$].[25] However, in each of these systems, the observed luminescence could be assigned entirely to transitions originating from just one, relatively isolated and well-defined electronic excited state. The emitting-state manifold in Δ-[Os(CG[6])(DMbpy)]$^{2+}$ is much more complicated.

Conclusion

Among the several kinds of structural chirality present in Δ-[Os(CG[6])(DMbpy)]$^{2+}$, that associated with the coordination core and chelate−ring system of the complex makes the dominant (and sign-determining) contributions to the chiroptical properties examined in this study. However, it appears that chiral moieties located outside the central chelate−ring system, in the noncoordinated parts of the CG[6] ligand, also make significant contributions to these properties. The clearest evidence of this is found in our comparisons between the CD/absorption results obtained for Δ-[Os(CG[6])(DMbpy)]$^{2+}$ vs Δ-[Os(bpy)$_3$]$^{2+}$, where it appears that the extrachromophoric parts of the CG[6] ligand make contributions that diminish the magnitudes of the observed $\Delta\epsilon$ and g_{ab} quantities.

The stereochemistry of the coordination core and chelate−ring structure in Δ-[Os(CG[6])(DMbpy)]$^{2+}$ is essentially identical to that of Δ-[Os(bpy)$_3$]$^{2+}$, and therefore, it is expected that the chiroptical properties of these two complexes should be very similar throughout the MLCT transition regions of their CD/absorption spectra. On a *qualitative* level, this expectation is quite compatible with experimental observation. The features observed in the CD/absorption spectra of Δ-[Os(CG[6])(DMbpy)]$^{2+}$ have shapes, relative intensities, sign patterns, and spacings that are nearly identical to those observed in the CD/absorption spectra of Δ-[Os(bpy)$_3$]$^{2+}$ (in solution). However, on a *quantitative* level, the CD/absorption spectra of the two complexes show significant differences. The MLCT transitions in Δ-[Os(CG[6])(DMbpy)]$^{2+}$ show larger molar absorptivities (ϵ), but somewhat smaller CD intensities ($\Delta\epsilon$) and absorption dissymmetry factors (g_{ab}), than the corresponding transitions in Δ-[Os(bpy)$_3$]$^{2+}$. This indicates that ligand structure outside the central coordination core and chelate−ring system of Δ-[Os(CG[6])(DMbpy)]$^{2+}$ exerts a significant influence on both the dipole strengths and rotatory strengths of the MLCT transitions. This influence most likely derives from a combination of (1) inductive effects on the π-electron charge distributions within the bipyridyl moieties of the CG[6] ligand and (2) direct (through-space) interactions between the C_6 bridging atoms and pinene moieties of the CG[6] ligand and the chromophoric electrons involved in the MLCT transitions. Given the length of the C_6 bridge in CG[6], it is unlikely that this bridge will produce any significant structural distortions or strain in the coordination core of Δ-[Os(CG[6])(DMbpy)]$^{2+}$. However, this bridge has a rigid and well-defined conformational chirality, and its direct interactions with the chromophoric electrons of the complex will almost certainly alter the degree of helicity associated with MLCT processes. Similarly, each of the two pinene moieties in the CG[6] ligand contains three asymmetric carbon atoms which may also alter the helicity of the force-fields acting on the chromophoric electrons.

In our earlier discussion of the absorption and emission dissymmetry factors observed for Δ-[Os(CG[6])(DMbpy)]$^{2+}$ in the CD−CPL spectral overlap region (15 000−13 000 cm^{-1}), we attributed the observed differences between the magnitudes of g_{ab} and g_{em} to chirality-related structural differences between the equilibrium ground state and ^{3}MLCT emitting states of the complex. It was further suggested that these ground- vs emitting-state structural differences correspond to twist-type distortions within the coordination core and chelate−ring system of the complex. However, it is also possible that the observed differences between $|g_{ab}|$ and $|g_{em}|$ may be due entirely to differential ground- vs excited-state perturbations exerted by the extrachromophoric parts of the complex. It is certainly reasonable to expect that the ^{3}MLCT excited states of the complex would be perturbed more strongly than the ground state by interactions with the pinene and C_6 bridging moieties of the CG[6] ligand. This follows from the fact that the ^{3}MLCT excited states are created by processes that move electron charge density away from the Os(II) atom and into regions closer to the pinene and C_6 bridging moieties of the CG[6] ligand.

Experimental Section

All of the spectroscopic measurements reported in this study were carried out on solution samples prepared by dissolving 1.288 mg of Δ-[Os(CG[6])(DMbpy)](PF$_6$)$_2$ in 4 mL of spectrophotometric-grade acetonitrile. The acetonitrile was purchased from J. T. Baker and subsequently refluxed over NaH and redistilled prior to its use as solvent. The Δ-[Os(CG[6])(DMbpy)](PF$_6$)$_2$ compound was prepared following methods and procedures analogous to those previously reported for the preparation of the corresponding ruthenium(II) compound.[9]

(25) Moran, D. M.; Metcalf, D. H.; Richardson, F. S. *Inorg. Chem.* **1992**, *31*, 819−825.

Unpolarized absorption spectra measurements were carried out using a Varian Cary Model 5E absorption spectrophotometer, and CD/absorption spectra were recorded with a Jasco Model J-720 CD/absorption spectrophotometer. All absorption and CD measurements were performed on solution samples at room temperature (∼293 K).

All luminescence measurements were carried out using a photon-counting chiroptical emission spectrophotometer constructed at the University of Virginia. These measurements were performed under *steady-state* excitation/emission detection conditions, with excitation provided by a CW argon ion laser (Coherent Innova-90) tuned to 488 nm. The 488 nm output of the laser was externally attenuated to ∼250 mW prior to entering the sample. The sample was contained in a cuvette held in contact with a thermostated cuvette holder, and the temperature of this cuvette holder was maintained at 293 K. The TL ($I = I_L + I_R$) and CPL ($\Delta I = I_L - I_R$) spectra were measured in 80 repeated scans over the course of four days. The TL spectra shown in this paper correspond to the collection of over 40 million photons at the peak wavenumber data point, with a spectral data interval of 2 nm. These spectra are not corrected for instrumental response, which gradually decreases by ∼50% over the region from 500 to 850 nm, beyond which the response abruptly decreases by over 99% for wavelengths longer than ∼850 nm. CD/absorption measurements were carried out before and after the CPL/TL scan to verify sample integrity. No sample degradation was observed under the conditions of our experiments.

Acknowledgment. This work was supported in part by NATO (Supramolecular Chemistry Special Programme Grant RV 950653 to A.C.) and the U.S. National Science Foundation (Grant CHE-9213473 to F.S.R.). The authors gratefully acknowledge discussions with Prof. Vincenzo Balzani.

IC9609012